Turkish Online Journal of Qualitative Inquiry (TOJQI)
Volume 11, Issue 02, June 2020: 1040-1052
DOI: https://doi.org/10.67145/nzx0gz88

Drainage Morphometry-Based Sub-Watershed Prioritization Of The Tapi River Basin (Trb) Using Geospatial Technologies

Mr. M. D. Phalke[1], J. B. Aghade[2]

[1]Assistant Professor, Department of Geology and Geo-Informatics, Shri Shivaji College of Arts, Commerce and Science, Akola, (MH), India
[2]Dr. B.A.M.U, Aurangabad (Maharashtra), India

Abstract:

The present study utilized drainage morphometry to characterize the sub-watersheds of the Tapi River Basin (TRB) and prioritize them for groundwater recharge, bank erosion, and flood hazard assessment. Streams were extracted from the 30 m Shuttle Radar Topography Mission (SRTM) Digital Elevation Model (DEM). From the same SRTM DEM, drainage density, lineament density, and slope maps were generated. Land use/land cover (LULC) was classified from the 10 m Sentinel-2 image. Furthermore, geological, geomorphological, and fault dataset were downloaded from the Bhukosh portal of the Geological Survey of India. The linear, areal, and relief parameters were calculated for nine sub-watersheds (SB1–SB9) using a geographic information system (GIS). The sub-watersheds varied significantly concerning the physical features, which affect the hydrological behavior of the watershed. In terms of groundwater potential, SB9, SB7, and SB3 were found to have the highest potential; while, the bank erosion and flood hazards were the highest in SB4, SB2. The sub-watersheds (SB7) and (SB9) were more vulnerable to climate change than others. Overall, a groundwater potential zone (GWPZ) map was prepared using seven thematic layers (geology, geomorphology, drainage density, lineament density, LULC, soil, and slope). The very good class, good class, moderate class, low class, and very low class were recorded by 5.03%, 51.36%, 18.99%, 13.73%, and 10.89% of the basin area, respectively. It is suggested to implement water management practices in such sub-watersheds to optimize groundwater potential, minimize erosion and flood hazards, and build resilience capacity against predicted climate change impacts in the TRB region.

KeyWord:
- Morphometric analysis
- Remote Sensing
- GIS
- Groundwater Potential Zone
- Tapi River Basin

1. Introduction:

Rivers are some of the most dynamic components of the hydrological cycle and the pattern of networks they create reflects the flux of water, sediment and energy through a landscape (Leopold et al., 1964; Gregory and Walling, 1973). Quantitative description of drainage networks began with Horton (1932, 1945) and continued with Strahler (1952, 1957, 1964), Miller (1953) and Schumm (1956) whose parameters now underlie most morphometric work. As morphometric properties reflect the conjoint effects of lithology, structure, relief and climate (Mesa, 2006), they can be used to infer a basin's hydrological response, flood susceptibility and its erosion potential (Patton and Baker, 1976; Pareta and Pareta, 2011). Measures of basin size and shape, the number and length of streams and the steepness of the land (Nautiyal, 1994; Magesh and Chandrasekar, 2014) allow for comparisons between sub-watersheds even when data on discharge and sediment load are sparse.Remote sensing and GIS have enabled faster and more consistent analyses. Drainage networks can be extracted from digital elevation models over large areas and combined with other thematic layers to rank sub-watersheds for soil and water conservation (Biswas et al., 1999; Chopra et al., 2005; Javed et al., 2009) or to delineate zones of groundwater potential (Krishnamurthy et al., 1996; Sreedevi et al., 2005). Work on the hard-rock terrains of peninsular India has shown that morphometric rankings correlate well with field evidence of runoff and erosion (Nag and Chakraborty, 2003; Vittala et al., 2004; Prakash et al., 2016; Rai et al., 2017; Singh et al., 2018).The Tapi River Basin is the second largest west-flowing basin of peninsular India after the Narmada (Jain et al., 2007). Rivers draining the Deccan uplands respond sharply to monsoon floods which carry large volumes of sediment and erode channel banks (Kale and Rajaguru, 1987; Baker and Kale, 1998; Kale, 2002). Much of the basin is semi-arid and recurrent drought (Preeti and Yadav, 2018) combined with heavy withdrawals of water for irrigation and industry have led to declines in groundwater levels in this part of India (Rodell et al., 2009). Changes in land use have affected runoff and channel behavior (Pizzuto et al., 2000) and these in turn have affected sedimentation, soil loss, flood occurrence and the siting of dams and reservoirs (Rai et al., 2017). Morphometric analysis provides a practical way in which to find the sub-watersheds facing the most pressure and to set priorities for their management (Prakash et al., 2016).The goals of this study are to (i) characterise the linear, areal and relief properties of the Tapi River Basin and its nine sub-watersheds; (ii) evaluate their relative potential for erosion, flooding and groundwater recharge; and (iii) to identify the sub-watersheds most in need of intervention. The results are intended to help water management planning and hazard mitigation in the basin.

2. Materials And Methods

Thematic maps and morphometric parameters were prepared from remote sensing data in a GIS environment, and the drainage network and the slope, aspect and drainage density maps derived from the SRTM DEM at 30 m resolution (Farr et al., 2007). Land use/land cover was mapped from Sentinel-2 multispectral imagery at 10 m resolution acquired in 2022 (Drusch et al., 2012; Chatziantoniou et al., 2017). Geological, geomorphological and fault layers were obtained from the Bhukosh geoportal of the Geological Survey of India, and lineaments were mapped and converted to a density surface following established practice (O'Leary et al., 1976; Sander, 2007). The basin was divided into nine sub-watersheds (SB1–SB9). Streams were ordered according to Strahler (1964), and the linear, areal and relief parameters reported in Section 4 were calculated with the standard relations of Gravelius (1914), Horton (1932, 1945), Smith (1950), Miller (1953), Schumm (1956), Melton (1957) and Strahler (1957, 1964). To assess groundwater potential, seven thematic layers (geology, geomorphology, drainage density, lineament density, LULC, soil and slope) were combined by overlay analysis in the GIS, following the approach of Krishnamurthy et al. (1996), Saraf and Choudhury (1998) and Jaiswal et al. (2003). The composite map.

3. Study Area

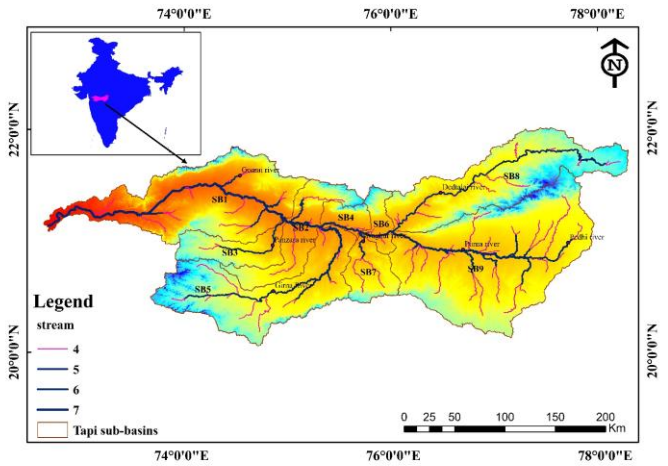

Figure 1: Location map of the Tapi River Basin

The Tapi River Basin is one of the major river basins of western India and, after the Narmada, the second largest basin of west-flowing rivers draining the Deccan Plateau. The basin is bounded by 72°33′E to 78°17′E longitude and 20°9′N to 21°50′N latitude and covers an area of about 65,145 km² (CWC and NRSC, 2014). The river originates from Satpura range in Betul district of Madhya Pradesh at an altitude of approximately 752 m above mean sea level and flows westwards through Madhya Pradesh, Maharashtra and Gujarat and finally discharge into the Arabian Sea near Surat (Jain et al., 2007). The river has four right-bank and ten left-bank tributaries of which nine are considered to be important; these include the Girna, Purna, Arunavati, Aner, Bori, Panzara, Waghur and Shillakhandi. Landforms within the basin range from the hills and ridges of the Satpura range which bounds it from the north to dissected plateaus and broad plains along the main valley (Preeti and Yadav, 2018). The climate is monsoonal characterised by summer temperatures, generally, ranging between 30 and 40 °C and winter temperatures between 15 and 25 °C, with an average annual rainfall of about 1000 mm with 85% of the rainfall recorded between June and September. Intensive monsoon rains may result in widespread flood while hot summers and dry monsoons could result in drought. The river provides water for domestic, agricultural, industrial and hydropower purposes and human activities such as deforestation, urban expansion and climate change are threatening water security in the basin.

4. Results And Discussion

4.1 Geology

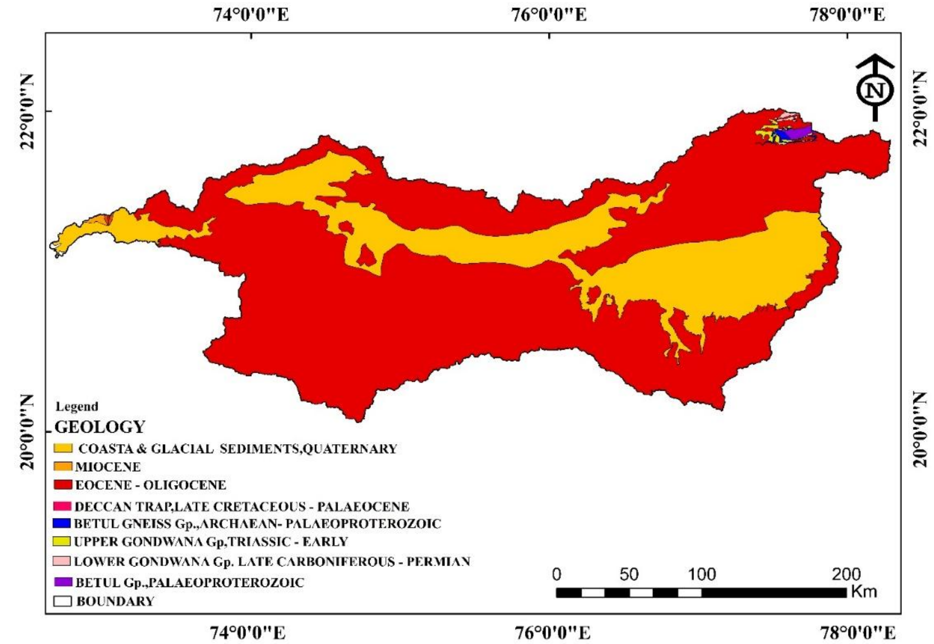

Figure 2: Geology map of the Tapi River Basin

The geology of the Tapi River Basin (Fig. 2; Table 1) is the product of a long and intricate tectonic development. The oldest rocks are of Precambrian age, consisting of gneisses and schists mainly exposed within the Satpura belt, which is part of the Central Indian Tectonic Zone (Acharyya and Roy, 2000). The Tapi valley lies on the southern margin of the SONATA (Son–Narmada–Tapi) lineament zone, a belt of old crustal weakness which has been reactivated several times, controlling much of the regional drainage (Jain et al., 1995; Acharyya and Roy, 2000). During the Mesozoic, India broke away from the rest of Gondwana and began its northwards drift (Storey et al., 1995; Chatterjee et al., 2013). Close to the Cretaceous–Paleogene boundary, about 66 million years ago, enormous quantities of basaltic lava flow erupted out of the Deccan Traps as a thick pile of basaltic flows (Beane et al., 1986; Courtillot et al., 1986; Schoene et al., 2015). These flows now underlie the greater part of the basin. The collision of India with Eurasia, which started some 50 million years ago (Patriat and Achache, 1984), placed the Indian plate under compression, rejuvenating older faults.

The youngest deposits are those of Quaternary alluvium consisting of sand, silt and clay deposited by the Tapi and its tributaries (Kale and Rajaguru, 1987). Late Quaternary uplift and incision have produced the present valleys, in much the same way as in the adjacent lower Narmada basin (Sant and Karanth, 1993). The basin is crossed by several east–west faults, including the Tapi and Gavilgarh faults (Section 4.4), while the Deccan region as a whole is subject to intraplate seismicity, exemplified by the 1993 Latur (Killari) earthquake (Seeber et al., 1996; Ray and Rao, 1998).

Table 1: Geology of the Tapi River Basin

Group	System	Rock Type	Localities	Age
Precambrian	Archean & Proterozoic	Gneisses and schists	Central and southern parts of the basin	1.5–2.5 (BY)
Paleozoic	Cambrian–Permian	Sandstones and shales	Central and northern parts of the basin	540–250 (MY)
Mesozoic	Triassic–Jurassic	Limestone and dolomite	Western and southern parts of the basin	250–145 (MY)
Cenozoic	Eocene–Pleistocene	Alluvial sediments	Alluvial plains of the basin	56–2 (MY)

4.2 Geomorphology

Geomorphology plays an important role in sub-watershed prioritization due to its control over runoff generation, erosion, sediment transport, and channel development. The Tapi River Basin encompasses structural hills, denudational uplands, pediplains, alluvial plains, river terraces, and valley fills that have evolved through the interaction of lithology, tectonics, and fluvial processes (Kale, 2002). The upper reaches are steep and deeply dissected, which promotes rapid runoff and erosion, whereas the middle and lower reaches are characterized by gentle slopes, wide valleys, and depositional landforms where sediment accumulates. Landforms have been mapped using satellite imagery, the DEM, and GIS-based terrain analysis. These techniques enable one to delineate landform units, analyze variations in slope and elevation, trace lineaments and drainage patterns, and correlate terrain with watershed behavior, and have been successfully used in comparable hard-rock terrains of peninsular India (Sreedevi et al., 2005; Magesh et al., 2011; Pareta and Pareta, 2015). In general, strongly dissected uplands and structurally controlled drainage indicate sub-watersheds with high runoff and a high risk of degradation, whereas low-relief alluvial tracts favor infiltration and deposition. Combined with morphometric parameters, it provides a more accurate ranking of sub-watersheds than either approach on its own.

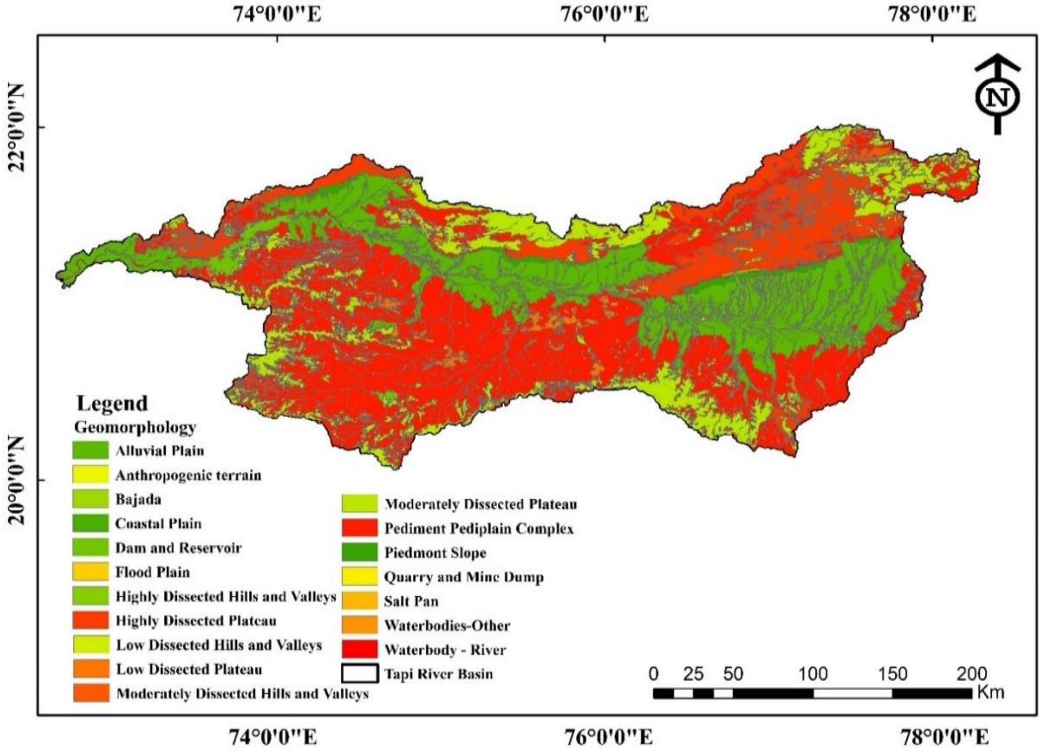

Figure 3: Geomorphology map of the Tapi River Basin

4.3 Land Use / Land Cover

The LULC map (Fig. 4) revealed that cropland is the dominant class followed by rangeland, water bodies, and built-up land that covered 65.43%, 27.26%, 3.34% and 3.34% of the basin, respectively. The other two classes (flooded vegetation and bare ground) were found to be less distributed in the basin and consisted 0.02% each. It can be seen that the classes were found to be unevenly distributed in the basin. The cropland was predominant in the central and southern parts while water bodies were mainly located in the eastern and northern parts of the basin. Built-up land was mostly distributed in the neighboring area of the big cities including Surat, Jalgaon, Dhule, Burhanpur, Akola and Amravati. On the other hand, the rangeland was dominantly located in the western and southern parts of the basin. Meanwhile, the patches of bare ground were found in the local dry areas. Since the land use cover has control on infiltration, runoff and sediment supply, these factors have a direct effect on channel stability and groundwater recharge (Pizzuto et al., 2000; Javed et al., 2009).

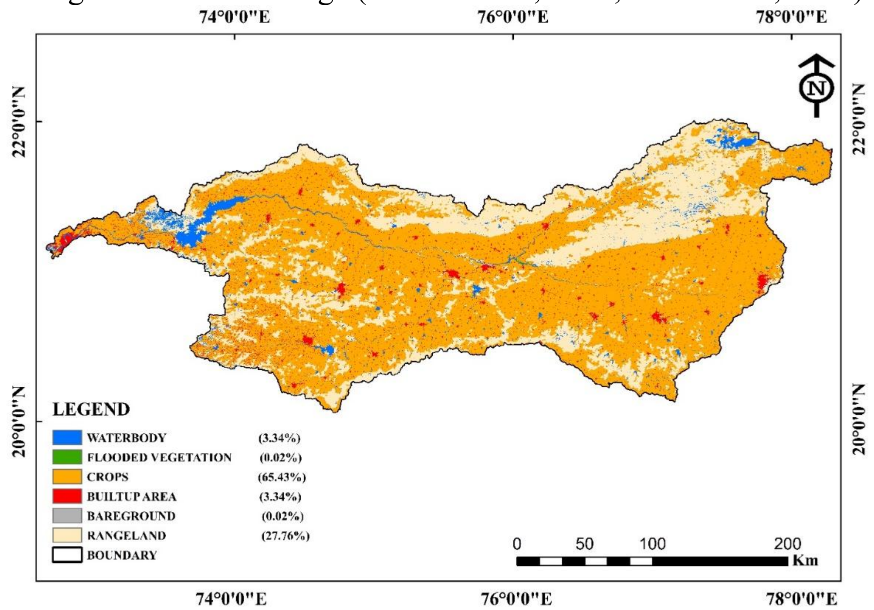

Figure 4: LULC map of the Tapi River Basin

4.4 Lineament Density

Lineament density was classified into five categories: very low, low, medium, high and very high (Figure 5). Three major faults were identified: the Tapi Fault, the Gavilgarh Fault and the Tapi North Fault. Lineaments are generally associated with zones of fracturing and jointing (O'Leary et al., 1976), and in hard-rock terrain such zones have been recognized as major pathways for infiltration and storage of groundwater (Jaiswal et al., 2003; Sander, 2007). Areas of high lineament density are therefore favorable for recharge and for drinking and irrigation supplies. Similarly, these structures control the development of streams and can concentrate runoff in fault-governed valleys (Nag and Chakraborty, 2003), which may increase erosion and flooding in the lower reaches.

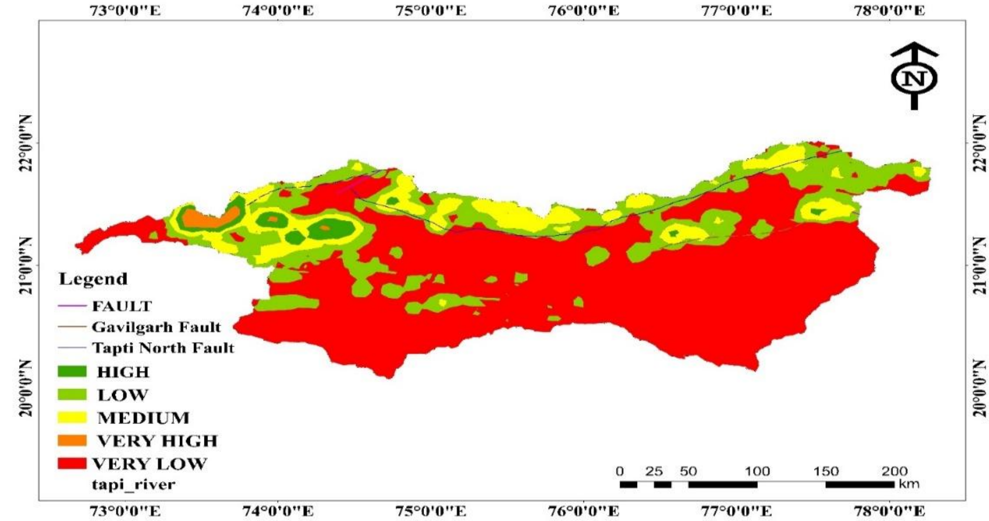

Figure 5: Lineament density and fault map of the Tapi River Basin

4.5 Morphometric Analysis

The morphometric analysis of a drainage basin comprises three groups of parameters: linear, areal and relief (Strahler, 1964). All three were used here to depict quantitatively the Tapi River Basin and rank its sub-watersheds.

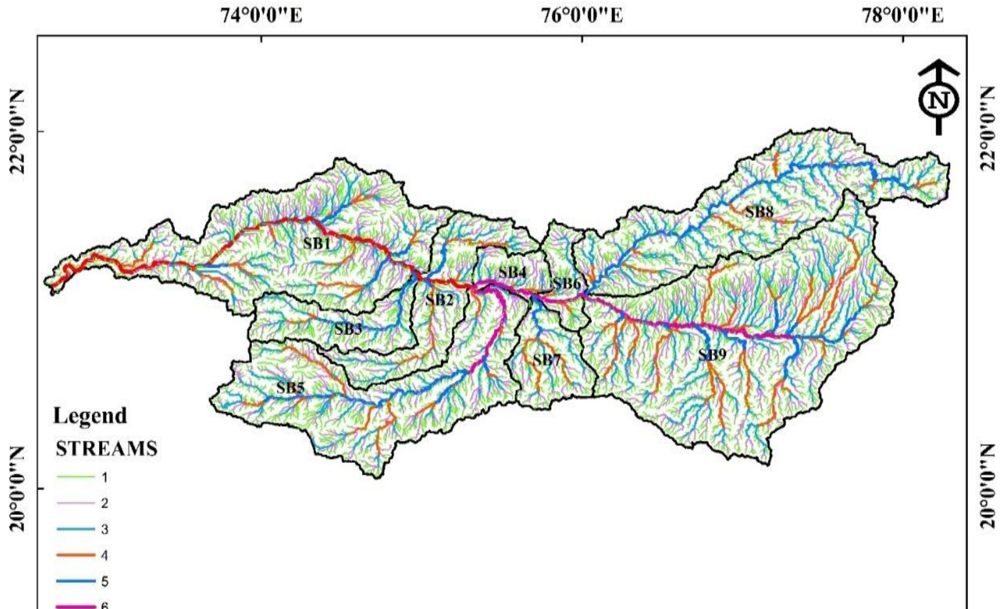

Figure 6: Stream order map of the Tapi River Basin

The streams in the nine sub-watersheds (SB1-SB9) were ordered according to the Strahler (1964) scheme (Table 2). The first-order streams account for 76.48% of total streams, followed by those of the second order (17.69%), while the third-order streams contribute 4.44%. The number of streams decreased consistently with increasing order according to Horton's (1945) law of stream numbers, and the stream network exhibited a dendritic pattern as a whole.

Stream Order	SB1	SB2	SB3	SB4	SB5	SB6	SB7	SB8	SB9	Total	%
1	1303	479	332	137	1068	140	255	1162	1767	6643	76.48
2	321	113	79	32	259	34	51	266	382	1537	17.69
3	86	22	19	8	59	7	12	72	101	386	4.44
4	19	6	1	2	15	2	2	14	26	87	1.00
5	5	3	1	1	3	1	1	1	8	24	0.27
6	1	1	0	1	1	1	0	0	1	6	0.06
7	0	1	0	1	0	0	0	0	0	2	0.02

Table 2: Stream order of the sub-basins of the Tapi River Basin (Σ total = 8,685 streams)

4.6 Linear Aspects

Linear parameters explain the one-dimensional characteristics of the drainage network, including the length, number, and arrangement of streams (Table 3). These parameters were calculated in GIS to identify the attributes of each sub-watershed's network and its influence on the runoff (Horton, 1945; Strahler, 1964). SB1 has the longest basin (265.00) and the greatest total stream length (7136.99), followed by SB8 and SB5, indicating large and well-developed networks that collect a considerable share of the basin's discharge. SB4, meanwhile, has the shortest basin (49.06), and SB4 and SB6 have the smallest total stream lengths, suggesting compact networks that contribute less to the basin's outflow. The bifurcation ratios range from 0.76 in SB8 to 3.23 in SB4; the higher values in SB4 and SB2 indicate some degree of structural control on the development of the drainage (Strahler, 1964; Nag and Chakraborty, 2003). Drainage density is highest in SB4 (0.65) and lowest in SB7 (0.50). Low drainage density typically reflects the permeability of the underlying material, the presence of good vegetation cover and low relief, which facilitates infiltration, while higher values are indicative of greater runoff and erosion (Strahler, 1964; Sreedevi et al., 2005). The stream frequency, length of overland flow and drainage texture also vary between sub-watersheds, reflecting differences in how quickly rainfall reaches the channels (Horton, 1945; Smith, 1950). Overall, the linear parameters highlight the different hydrological responses of the sub-watersheds, which is essential information for planning the use of the basin's water resources.

Table 3: Linear aspects of the sub-basins of the Tapi River Basin

SB	BL	TSL	LSM	BW	RB	LG	ER	DD	SF	RL	DT	CCM	SOR
SB1	265.00	7136.99	1.33	93.61	1.19	0.29	2.83	0.57	0.14	2.13	2.18	0.43	0.83
SB2	200.97	2267.05	1.32	35.18	2.53	0.26	5.71	0.53	0.14	0.60	1.17	0.47	0.39
SB3	130.26	1582.58	1.29	44.30	1.53	0.27	2.94	0.54	0.15	2.11	1.21	0.46	0.70
SB4	49.06	793.19	1.38	34.36	3.23	0.32	1.43	0.65	0.15	0.39	0.98	0.35	0.29
SB5	234.70	5385.13	1.31	58.06	1.25	0.27	4.04	0.53	0.14	1.78	1.99	0.47	0.82
SB6	68.59	783.30	1.34	31.08	2.23	0.29	2.21	0.58	0.14	0.49	0.82	0.42	0.42
SB7	65.22	1237.38	1.26	54.16	1.10	0.25	1.20	0.50	0.13	0.69	1.29	0.50	0.94
SB8	250.36	5437.23	1.30	60.56	0.76	0.26	4.13	0.51	0.14	1.54	2.04	0.49	1.32
SB9	235.67	1066.13	1.31	127.10	1.17	0.27	1.85	0.54	0.12	–	3.11	0.46	–

SB = sub- basin; BL = basal length; TSL = total stream length; LSM = length- slope factor/ mean stream length; BW = basin width; RB = bifur- cation ratio; LG = length of overland flow; ER = elongation ratio; DD = drainage density; SF = stream fre- quency; RL = stream length ratio; DT = drainage texture; CCM = constant of channel maintenance; SOR = stream order ratio.

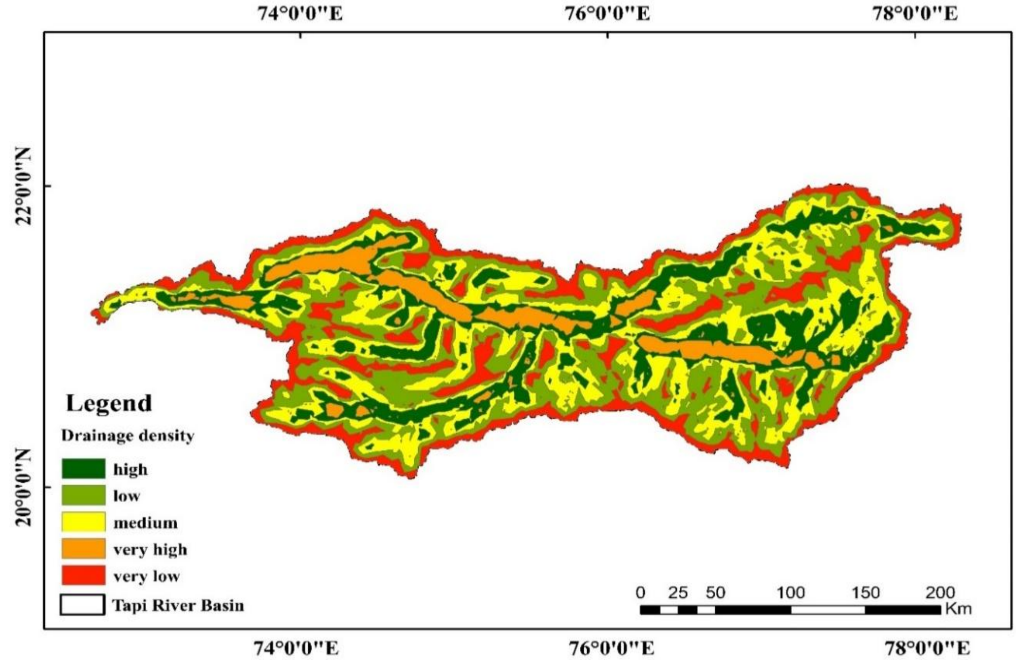

Figure 7: Drainage density map of the Tapi River Basin

4.7 Areal Aspects

Areal parameters define the size and shape of each sub-watershed that determine its response to rainfall including its susceptibility to drought and flooding (Table 4). SB9 has the largest area (18,585 km 2) while SB1 has the longest perimeter (797 km). SB9 also has relatively high values of circularity ratio, compactness coefficient and form factor plus the highest ruggedness number in the basin (0.54) indicating a fairly compact shape with a rugged terrain. The circularity ratio is highest in SB7 (0.50), followed by SB4 (0.45) and then SB9 (0.43). Near-circular basins tend to deliver runoff to the outlet quickly and produce sharper flood peaks while elongated basins with low circularity ratios such as SB2 (0.19) release runoff over a longer period (Horton, 1932; Miller, 1953; Schumm, 1956). SB4 has the smallest area (1,227 km 2) and perimeter (185 km) with intermediate values for the remaining parameters.

Table 4: Areal aspects of the sub-basins of the Tapi River Basin

SB	A	P	CR	CC	FF	Rn
SB1	12478	797	0.24685	0.02501	0.01964	0.50234
SB2	4317	536	0.18883	0.01913	0.01503	0.25316
SB3	2954	357	0.29126	0.02951	0.02318	0.27470
SB4	1227	185	0.45052	0.04565	0.03585	0.27285
SB5	10160	705	0.25688	0.02603	0.02044	0.45524
SB6	1360	226	0.33460	0.03390	0.02663	0.26356
SB7	2475	249	0.50163	0.05083	0.03992	0.24023
SB8	10593	741	0.24243	0.02456	0.01929	0.51328
SB9	18585	734	0.43349	0.04392	0.03450	0.54163

SB = sub-basin; A = area; P = perimeter; CR = circulatory ratio; CC = compactness coefficient; FF = form factor; Rn = ruggedness number.

4.8 Relief Aspects

Relief parameters indicate the vertical nature of a basin and explain its hydrological, erosional and ecological characteristics (Strahler, 1952; Schumm, 1956). Relief controls the velocity of runoff and the energy of erosion and so basins of greater overall relief and greater slopes tend to have higher flood peaks (Patton and Baker, 1976). The maximum, minimum and mean elevations, relief ratio, relative relief, longest flow path and valley depth of each of the sub-watersheds are given in table 5. SB5 has the highest maximum elevation (1563 m), highest mean elevation (905.50 m) and greatest valley depth (1420 m), so it is most mountainous sub-watershed with very deeply incised valleys and consequently fast runoff; its varied topography is likely to support a range of ecological niches. SB7 has lowest maximum (803 m) and mean (480.50 m) elevations and shallowest valley depth (649 m), and is flattest of the nine. Highest relief ratio is in SB1 (0.048) and highest relative relief in SB8 and SB9 (2.078). Longest flow paths occur in SB5, SB8 and SB1 and shortest in SB4. These differences in relief accounts for the differences in characteristics of runoff and erosion of the sub-watersheds.

Table 5: Relief aspects of the sub-basins of the Tapi River Basin

SB	Max E (m)	Min E (m)	Mean E (m)	Rr	RR	LFP	VD
SB1	1259	-21	640.03	0.048	1.99	339.58	1280
SB2	1039	114	576.95	0.025	1.60	253.88	925
SB3	1192	131	661.37	0.030	1.60	185.02	1061
SB4	1067	119	593.00	0.020	1.61	22.26	948
SB5	1563	143	905.50	0.030	1.56	357.21	1420
SB6	932	150	541.80	0.020	1.42	49.64	782
SB7	803	154	480.50	0.030	1.35	112.01	649
SB8	1088	-21	533.50	0.040	2.078	344.36	1109
SB9	1088	-21	533.50	0.030	2.078	333.75	1109

SB = sub-basin; Max E = maximum elevation; Min E = minimum elevation; Mean E = mean elevation; Rr = relief ratio; RR = relative relief; LFP = longest flow path; VD = valley depth.

5. Conclusion

The sub-watersheds of the Tapi River Basin are different from each other and have varying groundwater potential zones. From Figure 7, it can be seen that SB9, SB7 and SB3 have higher groundwater potential as indicated by their low drainage density and infiltration capacity. The groundwater potential map (Figure 8) was generated using seven input data layers; geology, geomorphology, drainage density, lineament density, LULC, soil and slope. The map shows that 5.03% of the basin falls under the very good category, 51.36% in good, 18.99% in moderate, 13.73% in low, and 10.89% in very low groundwater potential zones. It can be used to identify recharge zone areas within the sub-watersheds.

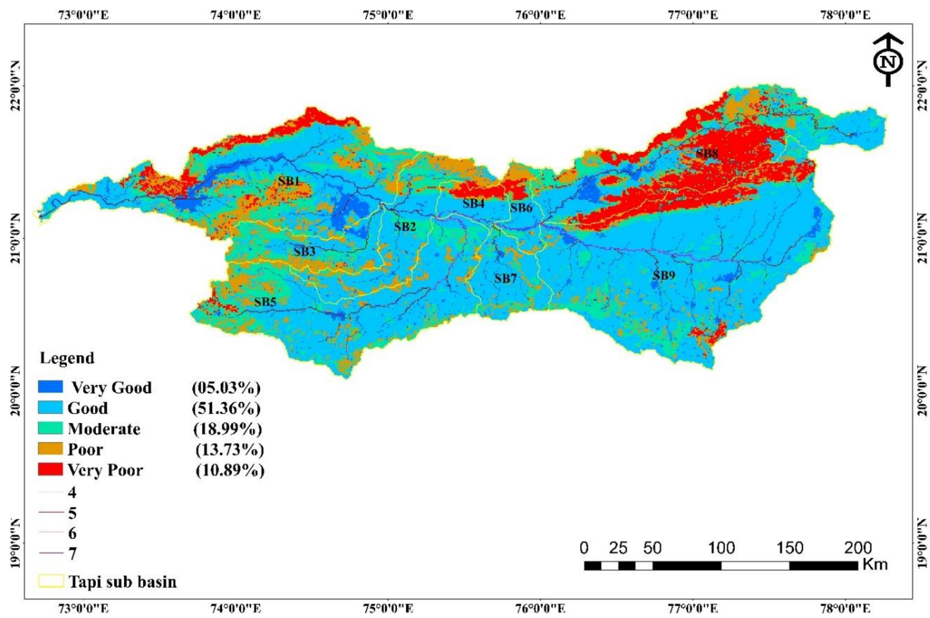

Figure 8: Groundwater Potential Zone (GWPZ) map of the Tapi River Basin

SB4 and SB2 are the most vulnerable to bank erosion and flooding due to the high drainage density and bifurcation ratio of SB4, and the high elongation and bifurcation ratios of SB2. SB7 and SB9 are the most reactive to climate change because of their high circularity ratios and, in the case of SB9, a large area. Thus, we suggest prioritizing the management of these sub-watersheds considering the identified hazards. In particular, the implementation of recharge structures in SB9 and SB7, as well as SB3, and the reduction of erosion and flooding in SB4 and SB2, should be prioritized. High priority should be given to sub-watersheds with high hazard levels. Overall, the current work highlights the importance of morphometric analysis combined with remote sensing and GIS technologies for assessing different hazards and implementing relevant management measures in large basins such as the Tapi basin.

References

1. Acharyya, S. K., & Roy, A. (2000). Tectonothermal history of the Central Indian Tectonic Zone and reactivation of major faults/shear zones. Journal of the Geological Society of India, 55(3), 239–256.
2. Baker, V. R., & Kale, V. S. (1998). The role of extreme floods in shaping bedrock channels. In K. J. Tinkler & E. E. Wohl (Eds.), Rivers Over Rock: Fluvial Processes in Bedrock Channels (Geophysical Monograph 107, pp. 153–165). American Geophysical Union.
3. Beane, J. E., Turner, C. A., Hooper, P. R., Subbarao, K. V., & Walsh, J. N. (1986). Stratigraphy, composition and form of the Deccan Basalts, Western Ghats, India. Bulletin of Volcanology, 48(1), 61–83.
4. Biswas, S., Sudhakar, S., & Desai, V. R. (1999). Prioritisation of subwatersheds based on morphometric analysis of drainage basin: A remote sensing and GIS approach. Journal of the Indian Society of Remote Sensing, 27(3), 155–166.
5. Chatterjee, S., Goswami, A., & Scotese, C. R. (2013). The longest voyage: Tectonic, magmatic, and paleoclimatic evolution of the Indian plate during its northward flight from Gondwana to Asia. Gondwana Research, 23(1), 238–267.
6. Chatziantoniou, A., Petropoulos, G. P., & Psomiadis, E. (2017). Co-orbital Sentinel 1 and 2 for LULC mapping with emphasis on wetlands in a Mediterranean setting based on machine learning. Remote Sensing, 9(12), 1259.
7. Chopra, R., Dhiman, R. D., & Sharma, P. K. (2005). Morphometric analysis of sub-watersheds in Gurdaspur district, Punjab using remote sensing and GIS techniques. Journal of the Indian Society of Remote Sensing, 33(4), 531–539.

8. Courtillot, V., Besse, J., Vandamme, D., Montigny, R., Jaeger, J. J., & Cappetta, H. (1986). Deccan flood basalts at the Cretaceous/Tertiary boundary? Earth and Planetary Science Letters, 80(3–4), 361–374.
9. CWC and NRSC (2014). Tapi Basin (Version 2.0). India-WRIS Project, Central Water Commission and National Remote Sensing Centre, Ministry of Water Resources, Government of India, New Delhi.
10. Drusch, M., Del Bello, U., Carlier, S., Colin, O., Fernandez, V., Gascon, F., Hoersch, B., Isola, C., Laberinti, P., Martimort, P., Meygret, A., Spoto, F., Sy, O., Marchese, F., & Bargellini, P. (2012). Sentinel-2: ESA's optical high-resolution mission for GMES operational services. Remote Sensing of Environment, 120, 25–36.
11. Farr, T. G., Rosen, P. A., Caro, E., Crippen, R., Duren, R., Hensley, S., Kobrick, M., Paller, M., Rodriguez, E., Roth, L., Seal, D., Shaffer, S., Shimada, J., Umland, J., Werner, M., Oskin, M., Burbank, D., & Alsdorf, D. (2007). The Shuttle Radar Topography Mission. Reviews of Geophysics, 45(2), RG2004. https://doi.org/10.1029/2005RG000183
12. Gravelius, H. (1914). Flusskunde (Grundriss der gesamten Gewässerkunde, Band 1). Göschen'sche Verlagshandlung, Berlin.
13. Gregory, K. J., & Walling, D. E. (1973). Drainage Basin Form and Process: A Geomorphological Approach. Edward Arnold, London.
14. Horton, R. E. (1932). Drainage-basin characteristics. Transactions, American Geophysical Union, 13(1), 350–361.
15. Horton, R. E. (1945). Erosional development of streams and their drainage basins: Hydrophysical approach to quantitative morphology. Geological Society of America Bulletin, 56(3), 275–370.
16. Jain, S. C., Nair, K. K. K., & Yedekar, D. B. (1995). Geology of the Son–Narmada–Tapti lineament zone in Central India. In Geoscientific Studies of the Son–Narmada–Tapti Lineament Zone, Project CRUMANSONATA (Geological Survey of India Special Publication 10, pp. 1–154).
17. Jain, S. K., Agarwal, P. K., & Singh, V. P. (2007). Hydrology and Water Resources of India (Water Science and Technology Library, Vol. 57). Springer, Dordrecht.
18. Jaiswal, R. K., Mukherjee, S., Krishnamurthy, J., & Saxena, R. (2003). Role of remote sensing and GIS techniques for generation of groundwater prospect zones towards rural development: An approach. International Journal of Remote Sensing, 24(5), 993–1008.
19. Javed, A., Khanday, M. Y., & Ahmed, R. (2009). Prioritization of sub-watersheds based on morphometric and land use analysis using remote sensing and GIS techniques. Journal of the Indian Society of Remote Sensing, 37(2), 261–274.
20. Kale, V. S. (2002). Fluvial geomorphology of Indian rivers: An overview. Progress in Physical Geography, 26(3), 400–433.
21. Kale, V. S., & Rajaguru, S. N. (1987). Late Quaternary alluvial history of the northwestern Deccan upland region. Nature, 325(6105), 612–614.
22. Krishnamurthy, J., Venkatesa Kumar, N., Jayaraman, V., & Manivel, M. (1996). An approach to demarcate ground water potential zones through remote sensing and a geographical information system. International Journal of Remote Sensing, 17(10), 1867–1884.
23. Leopold, L. B., Wolman, M. G., & Miller, J. P. (1964). Fluvial Processes in Geomorphology. W. H. Freeman, San Francisco.
24. Magesh, N. S., & Chandrasekar, N. (2014). GIS model-based morphometric evaluation of Tamiraparani subbasin, Tirunelveli district, Tamil Nadu, India. Arabian Journal of Geosciences, 7(1), 131–141.
25. Magesh, N. S., Chandrasekar, N., & Soundranayagam, J. P. (2011). Morphometric evaluation of Papanasam and Manimuthar watersheds, parts of Western Ghats, Tirunelveli district, Tamil Nadu, India: A GIS approach. Environmental Earth Sciences, 64(2), 373–381.
26. Melton, M. A. (1957). An Analysis of the Relations among Elements of Climate, Surface Properties, and Geomorphology (Technical Report 11, Project NR 389-042). Office of Naval Research, Department of Geology, Columbia University, New York.

27. Mesa, L. M. (2006). Morphometric analysis of a subtropical Andean basin (Tucumán, Argentina). Environmental Geology, 50(8), 1235–1242.
28. Miller, V. C. (1953). A Quantitative Geomorphic Study of Drainage Basin Characteristics in the Clinch Mountain Area, Virginia and Tennessee (Technical Report 3, Project NR 389-042). Office of Naval Research, Department of Geology, Columbia University, New York.
29. Nag, S. K., & Chakraborty, S. (2003). Influence of rock types and structures in the development of drainage network in hard rock area. Journal of the Indian Society of Remote Sensing, 31(1), 25–35.
30. Nautiyal, M. D. (1994). Morphometric analysis of a drainage basin using aerial photographs: A case study of Khairkuli basin, district Dehradun, U.P. Journal of the Indian Society of Remote Sensing, 22, 251–261. https://doi.org/10.1007/BF03026526
31. O'Leary, D. W., Friedman, J. D., & Pohn, H. A. (1976). Lineament, linear, lineation: Some proposed new standards for old terms. Geological Society of America Bulletin, 87(10), 1463–1469.
32. Pareta, K., & Pareta, U. (2011). Quantitative morphometric analysis of a watershed of Yamuna basin, India using ASTER (DEM) data and GIS. International Journal of Geomatics and Geosciences, 2(1), 248–269.
33. Pareta, K., & Pareta, P. U. (2015). Geomorphological interpretation through satellite imagery and DEM data. American Journal of Geophysics, Geochemistry and Geosystems, 1(2), 19–36.
34. Patriat, P., & Achache, J. (1984). India–Eurasia collision chronology has implications for crustal shortening and driving mechanism of plates. Nature, 311(5987), 615–621.
35. Patton, P. C., & Baker, V. R. (1976). Morphometry and floods in small drainage basins subject to diverse hydrogeomorphic controls. Water Resources Research, 12(5), 941–952.
36. Pizzuto, J. E., Hession, W. C., & McBride, M. (2000). Comparing gravel-bed rivers in paired urban and rural catchments of southeastern Pennsylvania. Geology, 28(1), 79–82. https://doi.org/10.1130/0091-7613(2000)28<79:CGRIPU>2.0.CO;2
37. Prakash, K., Mohanty, T., Singh, S., Chaubey, K., & Prakash, P. (2016). Drainage morphometry of the Dhasan River Basin, Bundelkhand Craton, central India, using remote sensing and GIS techniques. Journal of the Indian Society of Geomatics, 10(2).
38. Preeti, R., & Yadav, S. M. (2018). Spatiotemporal drought assessment of a semi-arid part of middle Tapi River Basin, India. International Journal of Disaster Risk Reduction, 28, 414–426.
39. Rai, P. K., Mohan, K., Mishra, S., & Ahmad, A. (2017). A GIS-based approach in drainage morphometric analysis of the Kanhar River Basin, India. Applied Water Science, 7, 217–232. https://doi.org/10.1007/s13201-014-0238-y
40. Ray, A. K., & Rao, K. K. (1998). Latur earthquake—Osmanabad area: A perspective analysis from remote sensing. In Space Informatics for Sustainable Development (p. 161).
41. Rodell, M., Velicogna, I., & Famiglietti, J. S. (2009). Satellite-based estimates of groundwater depletion in India. Nature, 460(7258), 999–1002. https://doi.org/10.1038/nature08238
42. Sander, P. (2007). Lineaments in groundwater exploration: A review of applications and limitations. Hydrogeology Journal, 15(1), 71–74.
43. Sant, D. A., & Karanth, R. V. (1993). Drainage evolution of the lower Narmada valley, western India. Geomorphology, 8(2–3), 221–244.
44. Saraf, A. K., & Choudhury, P. R. (1998). Integrated remote sensing and GIS for groundwater exploration and identification of artificial recharge sites. International Journal of Remote Sensing, 19(10), 1825–1841.
45. Schoene, B., Samperton, K. M., Eddy, M. P., Keller, G., Adatte, T., Bowring, S. A., Khadri, S. F. R., & Gertsch, B. (2015). U-Pb geochronology of the Deccan Traps and relation to the end-Cretaceous mass extinction. Science, 347(6218), 182–184. https://doi.org/10.1126/science.aaa0118
46. Schumm, S. A. (1956). Evolution of drainage systems and slopes in badlands at Perth Amboy, New Jersey. Geological Society of America Bulletin, 67(5), 597–646.

47. Seeber, L., Ekström, G., Jain, S. K., Murty, C. V. R., Chandak, N., & Armbruster, J. G. (1996). The 1993 Killari earthquake in central India: A new fault in Mesozoic basalt flows? Journal of Geophysical Research: Solid Earth, 101(B4), 8543–8560.
48. Singh, S., Kanhaiya, S., Singh, A., & Chaubey, K. (2018). Drainage network characteristics of the Ghaghghar River Basin (GRB), Son Valley, India. Geology, Ecology, and Landscapes. https://doi.org/10.1080/24749508.2018.1525670
49. Smith, K. G. (1950). Standards for grading texture of erosional topography. American Journal of Science, 248(9), 655–668.
50. Sreedevi, P. D., Subrahmanyam, K., & Ahmed, S. (2005). The significance of morphometric analysis for obtaining groundwater potential zones in a structurally controlled terrain. Environmental Geology, 47(3), 412–420.
51. Storey, M., Mahoney, J. J., Saunders, A. D., Duncan, R. A., Kelley, S. P., & Coffin, M. F. (1995). Timing of hot spot-related volcanism and the breakup of Madagascar and India. Science, 267(5199), 852–855.
52. Strahler, A. N. (1952). Hypsometric (area-altitude) analysis of erosional topography. Geological Society of America Bulletin, 63(11), 1117–1142.
53. Strahler, A. N. (1957). Quantitative analysis of watershed geomorphology. Transactions, American Geophysical Union, 38(6), 913–920.
54. Strahler, A. N. (1964). Quantitative geomorphology of drainage basins and channel networks. In V. T. Chow (Ed.), Handbook of Applied Hydrology (pp. 4-39–4-76). McGraw-Hill, New York.
55. Vittala, S. S., Govindaiah, S., & Honne Gowda, H. (2004). Morphometric analysis of sub-watersheds in the Pavagada area of Tumkur district, South India using remote sensing and GIS techniques. Journal of the Indian Society of Remote Sensing, 32(4), 351–362.